

doi: 10.15407/ujpe62.08.0666

V.S. STASCHUK,<sup>1</sup> V.G. KRAVETS,<sup>1</sup> V.O. LYSIUK,<sup>2</sup> O.P. POLYANSKA,<sup>1</sup>  
V.V. STUKALENKO,<sup>1</sup> A.L. YAMPOLSKY<sup>1</sup><sup>1</sup> Taras Shevchenko National University of Kyiv, Faculty of Physics

(4, Academician Glushkov Ave., Kyiv 03022, Ukraine; e-mail: svv@univ.kiev.ua)

<sup>2</sup> V.E. Lashkaryov Institute of Semiconductor Physics, Nat. Acad. of Sci. of Ukraine

(41, Nauky Ave., Kyiv 03028, Ukraine)

**STRUCTURE AND OPTICAL PROPERTIES  
OF  $(\text{Co}_{41}\text{Fe}_{39}\text{B}_{20})_x(\text{SiO}_2)_{1-x}$  NANOCOMPOSITES**PACS 71.20.Nr, 72.20.Pa

---

The ellipsometric parameters  $\Delta$  and  $\Psi$  for amorphous ferromagnetic alloys in the dielectric matrix,  $(\text{Co}_{41}\text{Fe}_{39}\text{B}_{20})_x(\text{SiO}_2)_{1-x}$ , have been measured in the spectral interval  $\lambda = 0.24 \div 1.0 \mu\text{m}$  ( $h\nu = 1.24 \div 5.15 \text{ eV}$ ) at various  $x$ -values. On the basis of the data obtained, the spectral dependences of the optical conductivity,  $\sigma(h\nu)$ , in those nanocomposites are studied. The dimensions of ferromagnetic particles were varied from 2 to 10 nm. The surface structure of nanocomposites is researched, by using scanning atomic force microscopy. The optical properties of nanocomposites are found to depend not only on the metal phase content, but also on the properties of interface regions, which are significantly different at metal phase contents above and below the percolation threshold.

*Keywords:* ferromagnetic alloys, ellipsometry, optical conductivity, interband transitions, percolation.

**1. Introduction**

The electric and magnetic properties of  $(\text{Co}_{41}\text{Fe}_{39}\text{B}_{20})_x(\text{SiO}_2)_{1-x}$  nanocomposites have currently been studied rather well [1–4]. To a certain extent, this is also true for their optical and magneto-optical properties [5–8]. However, the mechanism of light absorption by such complicated objects has not been elucidated in the cited works. The practical interest in metal nanocomposites in a dielectric matrix is caused by the prospects of their application as magnetic heads for the information recording and reproducing [3].

Amorphous magnetically soft alloys on the basis of iron and cobalt are widely used for the creation of magnetic recording heads. They have good magnetic

properties at low frequencies. However, in the high-frequency interval, their application becomes complicated owing to growing eddy-current losses [3]. It is evident that, in order to reduce those losses, it is necessary to increase the specific electric resistance of magnetic alloys.

One of the ways to solve this task is to apply composite nanostructured materials on the basis of amorphous ferromagnetic alloys with an insulator. Those composites consist of metal nano-sized granules that are chaotically distributed in a dielectric matrix [4]. Silicon or aluminum oxides are used as dielectric fillers. As a result, the specific electroresistance substantially increases and, accordingly, the frequency interval of applications of a magnetic material can be considerably extended.

The indicated nanocomposites are characterized by the high mechanical strength and corrosion resistance [8]. One should also take into account that nanocom-

---

© V.S. STASCHUK, V.G. KRAVETS, V.O. LYSIUK,  
O.P. POLYANSKA, V.V. STUKALENKO,  
A.L. YAMPOLSKY, 2017

posites are multiphase rather than diphas systems, so that they are characterized by a complicated electron structure [7–9]. In particular, it was found [10] that not only ions of  $d$ -metals  $\text{Fe}^{3+}$ ,  $\text{Fe}^{2+}$ , and  $\text{Co}^{2+}$  participate in the absorption in the X-ray interval, but also oxygen ions (they form oxides of transition metals), as well as silicon, and, to a less extent, boron ones.

The specific electrical resistance  $\rho$  of nanocomposites substantially depends on their content [3, 4]. In the content interval  $x = 0.35 \div 0.50$ , the specimens of  $(\text{Co}_{41}\text{Fe}_{39}\text{B}_{20})_x(\text{SiO}_2)_{1-x}$  composites reveal a smooth bend in the content dependence  $\rho(x)$ , which confirms conclusions of the percolation theory model [3] made for the case of zero conductivity in dielectric regions. For the composites concerned,  $(\text{Co}_{41}\text{Fe}_{39}\text{B}_{20})_x(\text{SiO}_2)_{1-x}$ , the percolation threshold value corresponds to the content  $x \approx 0.47$  [3, 4].

## 2. Specimen Fabrication and Measurement Procedures

Specimens of amorphous metal alloy–insulator composite nanostructures were fabricated in the argon atmosphere by sputtering a mixture of metal and dielectric components taken in the corresponding fractions with the help of an ion beam. They consisted of nanostructured granules of the amorphous ferromagnetic  $\text{Co}_{41}\text{Fe}_{39}\text{B}_{20}$  alloy inserted into an amorphous dielectric  $\text{SiO}_2$  matrix. The magnetic phase content was varied from 0.19 to 0.56. The thickness of nanocomposite films deposited onto glass substrates was approximately equal to  $1 \mu\text{m}$ . As a rule, this method of fabrication of specimens results in the size of ferromagnetic particles varying from 2 to 7 nm [10]. Hence, the structure of obtained nanocomposites comprised a set of inclusions of an amorphous metal alloy that were chaotically distributed over the amorphous dielectric matrix. Such a diphas (heterogeneous) structure is typical of not only the  $(\text{Co}_{41}\text{Fe}_{39}\text{B}_{20})_x(\text{SiO}_2)_{1-x}$  composites examined in this work, but also of other similar ones.

Spectral measurements of the ellipsometric parameters  $\Delta$  and  $\Psi$  were carried out in a wide spectral interval  $\lambda = 0.24 \div 1.0 \mu\text{m}$  ( $h\nu = 1.24 \div 5.15 \text{ eV}$ ) on a standard spectral ellipsometer Woollam M-2000. The optical properties of granular nanocomposites were studied, by using the reflection ellipsometry method. The choice of a measurement interval was done due to the strong absorption in this spectral re-

gion by nanocomposites with a high concentration of granules.

The essence of the method consists in the measurement of ellipsometric angles  $\Delta$  and  $\Psi$  at various photon energies  $h\nu$  and various incidence angles  $\phi$ . In the case of the simple model of a semiinfinite isotropic medium of the specimen in the medium with a real refractive index equal to 1 (air), the real,  $\varepsilon_1$ , and imaginary,  $\varepsilon_2$ , parts of the dielectric permittivity  $\tilde{\varepsilon} = \varepsilon_1 - i\varepsilon_2$  can be determined from the formulas [11]

$$\varepsilon_1 = a^2 - b^2 + \sin \varphi, \quad \varepsilon_2 = 2ab, \quad (1)$$

where

$$a = \sin \varphi \operatorname{tg} \varphi (1 - \operatorname{tg}^2 \Psi) / (1 + (\operatorname{tg} \Psi)^2 + 2 \operatorname{tg} \Psi \cos \Delta),$$

$$b = \sin \varphi \operatorname{tg} \varphi (2 \operatorname{tg} \Psi \sin \Delta) / (1 + (\operatorname{tg} \Psi)^2 + 2 \operatorname{tg} \Psi \cos \Delta), \quad (2)$$

$\varphi$  is the incidence angle,  $\Psi$  the azimuth of the restored linear polarization,  $\Delta$  the phase difference between the  $p$ - and  $s$ -components of the reflected light field strength. On the basis of the obtained relations (1) and (2), the optical conductivity can be determined, by using the expression  $\sigma = 2\pi\varepsilon_0\varepsilon_2\nu$ , where  $\varepsilon_0$  is the vacuum dielectric constant, and  $\nu$  the light frequency.

## 3. Results of Researches and Their Discussion

The spectral dependences of the ellipsometric parameters  $\Delta$  and  $\Psi$  in the spectral interval  $h\nu = 1.24 \div 5.15 \text{ eV}$  measured at various light incidence angles  $\phi = 55^\circ$ ,  $65^\circ$ , and  $75^\circ$  were used as raw data for researching the optical properties of nanocomposites. In Fig. 1, the dispersion curves of the ellipsometric parameters – the azimuth of the restored linear polarization,  $\Psi(\lambda)$ , and the phase difference,  $\Delta(\lambda)$  – for one of  $(\text{Co}_{41}\text{Fe}_{39}\text{B}_{20})_{0.59}(\text{SiO}_2)_{0.41}$  composite specimens are depicted. They were selected as initial for the calculation of optical characteristics of not only this composite, but also all other analyzed structures. One can see that the  $\Psi$ - and  $\Delta$ -values substantially depend not only on the wavelength  $\lambda$ , but also on the incidence angle  $\phi$ . The value of  $\Psi$  changes in the interval  $\Psi \approx 21 \div 34^\circ$ , whereas the value of  $\Delta$  changes in a much wider interval  $\Delta \approx 20 \div 150^\circ$ . However, it is known [11] that the measurement accuracy of the ellipsometric parameters  $\Delta$  and  $\Psi$  (and, therefore, the

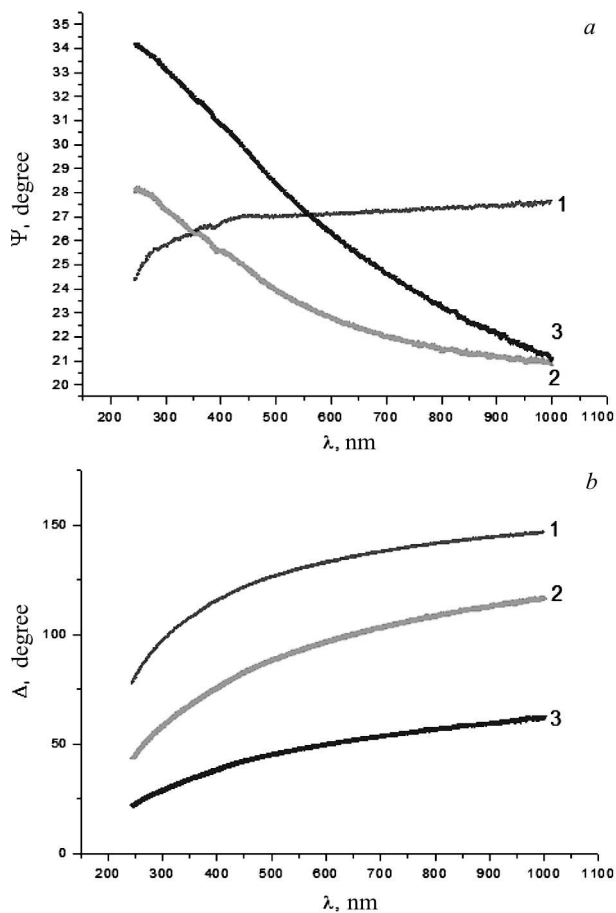


**Fig. 1.** Dispersion dependences of the azimuth of the restored linear polarization  $\Psi$  (a) and the phase difference  $\Delta$  (b) for the  $(\text{Co}_{41}\text{Fe}_{39}\text{B}_{20})_{0.41}(\text{SiO}_2)_{0.59}$  nanocomposite at the incidence angles  $\phi = 55^\circ$  (1),  $65^\circ$  (2), and  $75^\circ$  (3)

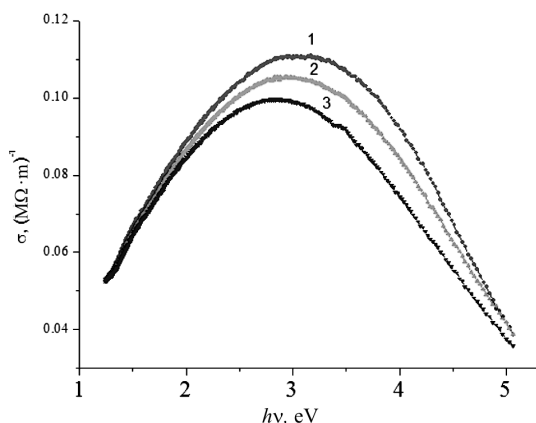


**Fig. 2.** Spectral dependences of the optical conductivity  $\sigma(h\nu)$  in the amorphous alloy  $\text{Co}_{41}\text{Fe}_{39}\text{B}_{20}$  at various incidence angles  $\phi = 55^\circ$  (1),  $65^\circ$  (2), and  $75^\circ$  (3)

optical constants  $n$  and  $\kappa$ ) is the highest for the principal angle of incidence  $\Phi$ , when the value of  $\Delta$  equals  $90^\circ$ . Therefore, below, we will analyze only the data that correspond to this criterion.

As is seen from Fig. 1, the principal angle of incidence for the given specimen at a wavelength approximately in the middle of the examined spectral interval equals  $\Phi = 65^\circ$ . Almost the same result was obtained for other structures. Therefore, only the data for this incidence angle will be analyzed below. The results of experimental researches for specimens with various  $x$  testify that the dispersion character of the quantities  $\Delta(\lambda)$  and  $\Psi(\lambda)$  considerably depends on the dielectric matrix fraction and the size of nanogranules of amorphous metal inclusions. This fact is associated with modifications in the structure of atomic (ionic) system and, to a larger extent, with changes in the electron structure of composites due to the variation of the metal phase content.

Of course, the most important are the spectral dependences of the optical conductivity,  $\sigma(h\nu)$ , obtained from the spectral dependences of ellipsometric parameters,  $\Delta(\lambda)$  and  $\Psi(\lambda)$ , for all studied specimens. In Fig. 2, the spectral dependences of the optical conductivity  $\sigma(h\nu)$  are shown for the amorphous metal alloy  $\text{Co}_{41}\text{Fe}_{39}\text{B}_{20}$ , of which the metal granules in all measured specimens were made. The dependence were obtained for the incidence angles  $\phi = 55^\circ$ ,  $65^\circ$ , and  $75^\circ$ . One can see that the character of the  $\sigma(h\nu)$  dispersion at various incidence angles is almost identical. At the same time, the dependence maximum becomes a little shifted toward longer waves, as  $\phi$  increases. This maximum emerges owing to the superposition of the Fe absorption occurring due to electron transitions mainly in a vicinity of points P and N in the Brillouin zone of iron and the absorption associated with transitions from the ground electron states of iron to the impurity states of cobalt [11]. A comparison between the results depicted in Fig. 2 and the data of work [12] obtained for massive Fe–Co alloys testifies that the absorption character is determined by the nearest environment. The latter practically does not change at the amorphization in Fe–Co–B compounds as compared with that in  $\text{Fe}_{50}\text{Co}_{50}$  crystal structures. At the same time, we may assert that metal compounds of iron and cobalt borides do not play a substantial role in the light absorption.

Finally, a certain distinction between the results corresponding to different incidence angles is induced

by the influence of near-surface layers, which are most likely composed of iron and cobalt oxides. The most reliable data correspond to the incidence angle  $\phi = 65^\circ$ , because, as was marked above, it is close to the principal one for a wavelength in about the middle of the examined spectral interval. Therefore, as was marked above, only the dispersion curves of the optical conductivity  $\sigma(h\nu)$  obtained for this incidence angle should be analyzed. That is why the dispersion curves of the optical conductivity  $\sigma(h\nu)$  obtained for  $(\text{Co}_{41}\text{Fe}_{39}\text{B}_{20})_x(\text{SiO}_2)_{1-x}$  nanocomposites with various  $x$ -values but only the incidence angle  $\phi = 65^\circ$  are exhibited in Fig. 3. From this figure, one can see that the dispersion character observed at the contents of the amorphous phase granules higher than the percolation threshold,  $x = 0.56$ , considerably changes when passing to lower contents ( $x = 0.41$  and  $0.33$ ). At an even lower content ( $x = 0.19$ ), when the granules are isolated from one another, the absorption is mainly caused by the  $\text{SiO}_2$  matrix.

Now, let us consider some results obtained for the optical properties (the dispersion of the optical conductivity  $\sigma(h\nu)$ , which is proportional to the inter-band density of states  $G(E)$ ) in the cases where the granule concentration is higher ( $x = 0.56$ ) and lower ( $x = 0.41$ ) than the percolation threshold (see Fig. 3), and at energies  $h\nu > 3.5$  eV. One can see that the absorption decreases in this interval (especially at  $x = 0.41$  at.%). Considerable changes are observed in the long-wave section of absorption spectra, where the main absorption bands of Fe (2.2–2.6 eV) and Co (0.8–1.3 eV) [11] associated with 3d-bands are located. In addition, interference effects manifest themselves in thin nanocomposite films. This effect is the most pronounced in specimens with a low concentration of magnetic phase characterized by a low absorption coefficient. The optical properties of composites were found to be mainly governed by properties of the metal phase at low  $\text{SiO}_2$  contents, and by properties of both the metal and amorphous  $\text{SiO}_2$  phases at high  $\text{SiO}_2$  contents. It should be noted that a certain displacement of the curves  $\sigma(h\nu)$  along the coordinate axes is observed for the same specimens but at various incidence angles (see Fig. 3), which undoubtedly testifies to the influence of the near-surface layer.

The main feature in spectral dependences of the optical conductivity  $\sigma(h\nu)$  is their distinct structuring in the energy interval lower than 2.5 eV at magnetic

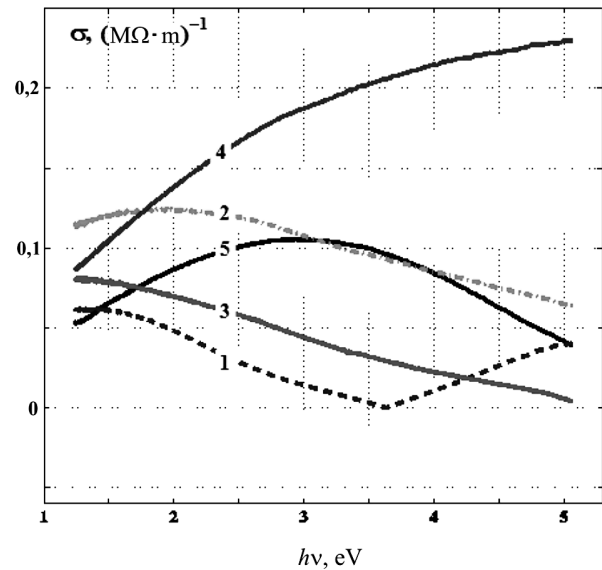


**Fig. 3.** Spectral dependences of the optical conductivity  $\sigma(h\nu)$  in  $(\text{Co}_{41}\text{Fe}_{39}\text{B}_{20})_x(\text{SiO}_2)_{1-x}$  nanocomposites with various  $x = 0.56$  (1), 0.41 (2), 0.33 (3), 0.19 (4), and 1 (5) at the incidence angle  $\phi = 65^\circ$

phase contents higher than 0.41. In our opinion, the presence of the intensive absorption in this region is associated with a substantial contribution of atomic electrons that are located near the granule surface to the optical conductivity in comparison with the contribution made by deep atomic electrons, whose concentration decreases with increase in the dielectric matrix fraction. We believe that this conclusion is also confirmed by the results of researches concerning the dispersion dependences of the residual optical conductivity in composites,

$$\Delta\sigma(h\nu) = \sigma_e(h\nu) - x\sigma_{\text{met}}(h\nu),$$

where  $\sigma_e$  is the experimental value of optical conductivity in a composite,  $\sigma_{\text{met}}$  the experimental values of conductivity in the metal phase, and  $x$  the metal phase content. The spectral dependences of the residual optical conductivity  $\Delta\sigma(h\nu)$  in the examined nanocomposites obtained for the incidence angle  $\phi = 65^\circ$  are depicted in Fig. 4.

In our opinion, the chemical admixtures of oxygen and silicon do not substantially affect the dispersion dependences of both the optical conductivity  $\sigma(h\nu)$  and the residual optical conductivity  $\Delta\sigma(h\nu)$  of studied composites at low dielectric matrix contents. The attention is attracted by a similarity between the dispersion dependences of the

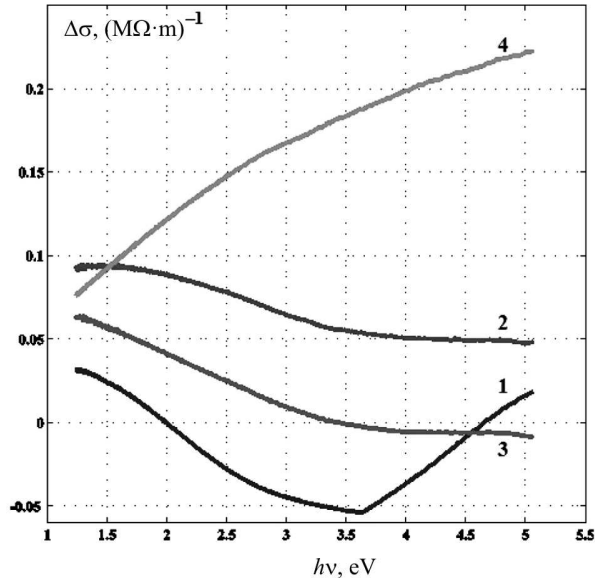


**Fig. 4.** Spectral dependences of the residual optical conductivity  $\Delta\sigma(h\nu)$  in  $(\text{Co}_{41}\text{Fe}_{39}\text{B}_{20})_x(\text{SiO}_2)_{1-x}$  nanocomposites with  $x = 0.56$  (1), 0.41 (2), 0.33 (3), and 0.19 (4) at the incidence angle  $\phi = 65^\circ$

residual optical conductivity  $\Delta\sigma(h\nu)$  obtained for the granule contents more than  $x = 0.33$ . Furthermore, at  $x = 0.56$ , almost all  $\Delta\sigma$  values are negative ( $\Delta\sigma < 0$ ). This fact testifies to a decay of those phases in the ferromagnetic structure of this composite, which are optically less active in comparison with this structure. At the same time, since the granules are rather big, the role of surface phenomena occurring at the interfaces between various phases is insignificant in comparison with the bulk phenomena. At the contents  $x = 0.33$  and 0.41, the size of ferromagnetic granules diminishes, and the role of the interface phenomena increases, which is associated with the formation of new silicide and oxide phases of both iron and cobalt. Note that the phases of iron and cobalt silicides are optically more active [11], and the absorption in them grows with a reduction of the photon energy  $h\nu$ . At the same time, in the specimen with the minimum content  $x = 0.19$ , the absorption grows together with the photon energy, which testifies to a considerable growth of the absorption in the amorphous  $\text{SiO}_2$  matrix. Furthermore, in the energy interval below 2.5 eV, the specimens are partially transparent. At the same time, the optical properties of this nanocomposite in the higher-energy interval are also governed

by interband transitions of electrons in the interface region.

#### 4. Conclusions

1. To summarize, we have found that the researched  $(\text{Co}_{41}\text{Fe}_{39}\text{B}_{20})_x(\text{SiO}_2)_{1-x}$  nanostructures are diphasic, i.e. heterogeneous, and their optical properties depend not only on the properties of two constituent phases, but also on the properties of interfaces in those structures (the interface regions).

2. Despite that the granules of the ferromagnetic phase have a complicated phase composition, their optical properties are mainly governed by interband electron transitions in Fe nanoclusters and Fe-Co clusters with an approximately equiatomic composition.

3. The optical properties of nanocomposites substantially depend on the metal phase content. This dependence is essentially different near the percolation threshold and below it.

1. F.F. Yang, S.S. Yan, M.X. Yu, Y.Y. Dai, S.S. Kang, Y.X. Chen, S.B. Pan, J.L. Zhang, H.L. Bai, T.S. Xu, D.P. Zhu, S.Z. Qiao, G.L. Liu, L.M. Mei. High-frequency electromagnetic properties of compositionally graded FeCoB-SiO<sub>2</sub> granular films deposited on flexible substrates. *J. Appl. Phys.* **111**, 113909 (2012).
2. A.V. Shchekochikhin, E.P. Domashevskaya, S.I. Karpov. Influence of the elemental composition on the basis of CoFeB-SiO<sub>2</sub> on nonmagnetic and magneto-resistive properties. *Kond. Sredy Mezhfaz. Gran.* **8**, 1 (2006) (in Russian).
3. I.V. Zolotukhin, Yu.E. Kalinin, O.V. Stognei. Granular magnetic materials. *Nanosyst. Nanomater. Nanotekhnol.* **2**, 1 (2004) (in Ukrainian).
4. P. Johnsson, S.-I. Aouqi, A.M. Grishin, M. Munakata. Transport anisotropy in hetero-amorphous (CoFeB)-SiO<sub>2</sub> thin films. *J. Appl. Phys.* **93**, 8101 (2003).
5. A.M. Kalashnikova, V.V. Pavlov, R.V. Pisarev, Yu.E. Kalinin, A.V. Sitnikov, Th. Rasing. Optical and magneto-optical properties of CoFeB/SiO<sub>2</sub> and CoFeZr/Al<sub>2</sub>O<sub>3</sub> granular magnetic nanostructures. *Phys. Solid State* **46**, 2163 (2004).
6. A.V. Shchekochikhin, E.P. Domashevskaya, S.I. Karpov, O.V. Stognei. Infrared spectra of amorphous nanocomposites and their interatomic interactions. *Kond. Sredy Mezhfaz. Gran.* **11**, 78 (2009) (in Russian).
7. E.A. Gan'shina, M.V. Vashuk, A.N. Vinogradov et al. Evolution of optical and magneto-optical properties in amorphous metal-insulator nanocomposites. *Zh. Èksp. Teor. Fiz.* **125**, 1172 (2004).

8. A.M. Kalashnikova, V.V. Pavlov, R.V. Pisarev *et al.* Optical and magneto-optical properties of granular magnetic nanostructures  $\text{CoFeB}/\text{SiO}_2$  and  $\text{CoFeZr}/\text{Al}_2\text{O}_3$ . *Fiz. Tverd. Tela* **46**, 2092 (2004) (in Russian).
9. Y. Wang, X.X. Zhang, X Yan *et al.* Study of optical properties of metallic  $\text{Au}_x(\text{SiO}_2)_{1-x}$  and  $\text{Ni}_x(\text{SiO}_2)_{1-x}$  films. *Physica B* **279**, 113 (2000).
10. E.P. Domashevskaya, S.A. Starozhilov, S.Yu. Turishchev *et al.* XANES and USXES studies of interatomic interactions in  $(\text{Co}_{41}\text{Fe}_{39}\text{B}_{20})_x(\text{SiO}_2)_{1-x}$  nanocomposites. *Fiz. Tverd. Tela* **50**, 135 (2008) (in Russian).
11. L.V. Poperenko, Yu.V. Kudryavtsev, V.S. Staschuk *et al.* *Optics of Metal Structures* (Kyiv University Publ. Center, 2013) (in Ukrainian).
12. V.S. Staschuk, A.N. Kravchuk. Optical properties of the electron structure in Fe–Co alloys. *Ukr. Fiz. Zh.* **34**, 1246 (1989) (in Ukrainian).

Received 31.01.17.

Translated from Ukrainian by O.I. Voitenko

*В.С. Стащук, В.Г. Кравець, В.О. Лисюк,  
О.П. Полянська, В.В. Стукаленко, А.Л. Ямпольський*

ОПТИЧНІ ВЛАСТИВОСТІ І СТРУКТУРА  
НАНОКОМПОЗИТІВ  $(\text{Co}_{41}\text{Fe}_{39}\text{B}_{20})_x(\text{SiO}_2)_{100-x}$

Резюме

В роботі на основі виміряних в спектральному інтервалі  $\lambda = 0,24\text{--}1,0$  мкм ( $h\nu = 1,24\text{--}5,15$  еВ) еліпсометричних параметрів  $\Delta$  та  $\Psi$  досліджено спектральні залежності оптичної провідності  $\sigma(h\nu)$  аморфних феромагнітних сплавів в діелектричній матриці  $(\text{Co}_{41}\text{Fe}_{39}\text{B}_{20})_x(\text{SiO}_2)_{100-x}$  при різних значеннях  $x$ . Розміри феромагнітних частинок змінювалися в інтервалі приблизно від 2 до 10 нм. Структурні дослідження наноконкомпозитів проводилося за допомогою скануючого атомно-силового мікроскопа. Встановлено, що оптичні властивості наноконкомпозитів при різних концентраціях металеві фази залежать не лише від долі цієї фази, а й від властивостей інтерфейсних областей, і ці властивості суттєво різні при концентраціях, вищих і нижчих порогу перколяції.